The study of protein mechanics with the atomic force microscope

Thomas E. Fisher, Andres F. Oberhauser, Mariano Carrion-Vazquez, Piotr E. Marszalek and Julio M. Fernandez

The unfolding and folding of single protein molecules can be studied with an atomic force microscope (AFM). Many proteins with mechanical functions contain multiple, individually folded domains with similar structures. Protein engineering techniques have enabled the construction and expression of recombinant proteins that contain multiple copies of identical domains. Thus, the AFM in combination with protein engineering has enabled the kinetic analysis of the force-induced unfolding and refolding of individual domains as well as the study of the determinants of mechanical stability.

PROTEIN–PROTEIN INTERACTIONS are responsible for maintaining the structural stability of cells and tissues[1,2] and for the generation of movement in processes such as muscle contraction, organelle transport and vesicular secretion. Proteins are thus responsible for a wide variety of mechanical functions, yet the physical properties underlying these functions are largely unknown. One common feature of many mechanical proteins is that they contain multiple, individually folded protein domains. Two important examples are the immunoglobulin (Ig)-type fold and the fibronectin-type fold (the most common of which is fibronectin type 3 or FN-III). Both are so-called β-sandwich structures and are found in a variety of proteins; the latter is present in an estimated 2% of all animal proteins[3]. These domains might unfold and refold as proteins execute mechanical functions. Force-induced extension of the protein titin, for example, which is responsible for the passive elasticity of muscle, can cause its constituent Ig and FN-III domains to unravel[4]. Individual molecules of the extracellular matrix (ECM) protein fibronectin can contract to less than one quarter of their original length when the ECM is disrupted, which suggests that the molecules were under strain and that some of the FN domains had been unfolded[5]. Unfolding and refolding of domains, as part of a particular mechanical function, could be a mechanism by which tension is maintained as a protein is extended or relaxed. Unfolding might also contribute to the function of fibronectin by exposing cryptic protein interaction sites that are important in ECM assembly[6–9].

Domain unfolding can be thought of as a two-state process in which the rate of conversion depends exponentially on the product of the axial force and the distance over which this force is applied (Fig. 1a). For a given mechanical stability, the force of unfolding will be high if disruption of the fold requires little extension, and will be lower if the forces maintaining the fold are distributed over a greater unfolding distance. The force required to unfold a domain is therefore highly dependent on the topology of the bonds in the fold. The location and strength of these bonds determine not only the mechanical stability, but also the dependence of the rates of unfolding and refolding on the applied force. These properties could be crucial to the physiological function of mechanical proteins. This review discusses recent developments in atomic force microscopy that permit precise measurement of the force-induced unfolding of single protein domains and that offer a new perspective on the function of proteins exposed to stretching forces.

T. E. Fisher, A. F. Oberhauser, M. Carrion-Vazquez, P. E. Marszalek and **J. M. Fernandez** are at the Dept of Physiology and Biophysics, Mayo Foundation, 1-117 Medical Sciences Building, Rochester, MN 55905, USA.
Email: fernandez.julio@mayo.edu

Single-molecule force spectroscopy

In the force-measuring mode of the atomic force microscope (AFM)[10–12], a single molecule is stretched between the microscopic silicon nitride tip of a flexible cantilever and a flat substrate that is mounted on a highly accurate piezoelectric positioner (Fig. 1b). A layer of protein, or other biological polymer, is either adsorbed to the substrate or linked to it through the formation of covalent bonds. When the tip and substrate are brought together and then withdrawn, one or more molecules can attach to the tip by adsorption. As the distance between the tip and substrate increases, extension of the molecule generates a restoring force that causes the cantilever to bend. This causes deflection of a laser beam directed toward the upper surface of the cantilever, which is measured using a photodetector. The output of the photodetector can be related to the angle of the cantilever and therefore to the applied force, if the elastic properties of the cantilever are known. This system allows spatial manipulations of less than a nanometer and can measure forces of a few piconewtons (pN).

Entropic elasticity

When a polymer is relaxed, it forms a coiled structure because this maximizes the entropy of its segments. Extension of the polymer generates an opposing force due to the reduction in entropy. This phenomenon, referred to as entropic elasticity, suggests that small extensions require little force but that the resistance to extension rises rapidly as the polymer approaches its full length. The behaviour of polymers under mechanical stress is described by the worm-like chain (WLC) model of elasticity[13–15]. This model describes a polymer as a continuous string of a given total (or contour) length (Fig. 2a). Bending of the polymer at any point influences the angle of the polymer for a distance, referred to as the persistence length, that reflects the polymer flexibility. The smaller the persistence length, the greater the entropy of the polymer and the greater the resistance to extension. The persistence length and the contour length comprise the adjustable parameters of the WLC model.

0968–0004/99/$ – See front matter PII: S0968-0004(99)01453-X

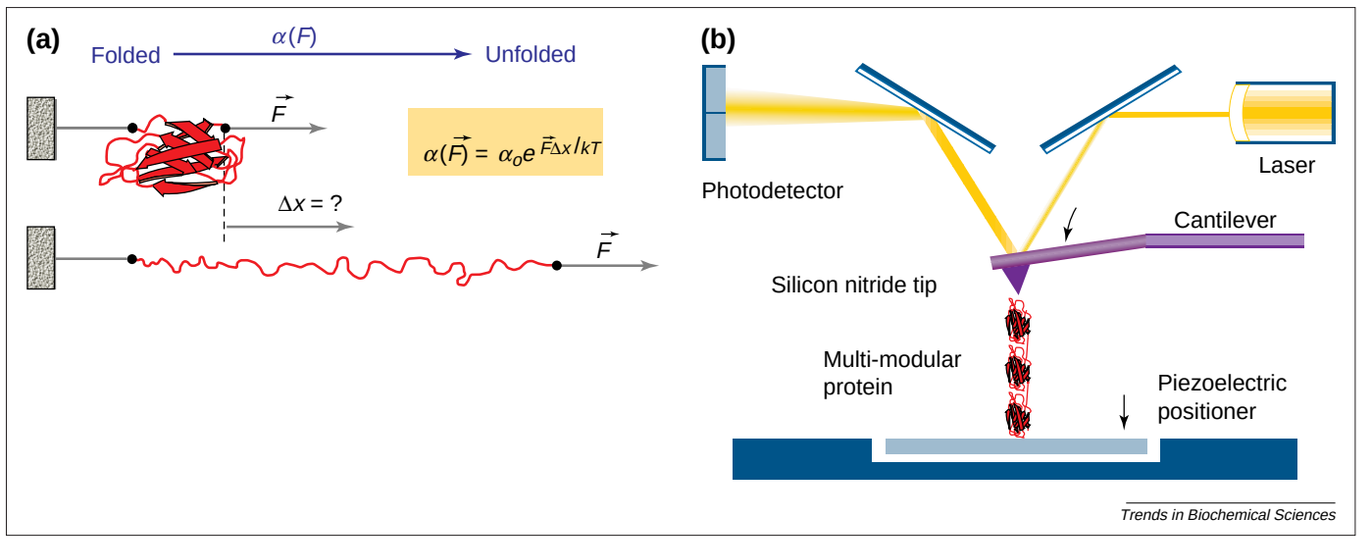

Figure 1

The unfolding of protein domains by an external force. **(a)** When axial stress is applied to a folded domain the protein will unravel. The inset shows an equation describing this transition, where F is the applied force, Δx is the distance over which the unfolding event occurs, α_0 is the rate constant in the absence of an applied force, k is Boltzmann's constant and T is the absolute temperature. Thus, the rate at which protein unfolding occurs increases exponentially with the applied force. This equation is similar to that describing the dissociation of non-covalent bonds placed under an external force[38,39]. **(b)** The force–extension mode of the atomic force microscope (AFM). When pressed against a layer of protein attached to a substrate, the silicon nitride tip can adsorb a single protein molecule. Extension of a molecule by retraction of the piezoelectric positioner results in deflection of the AFM cantilever. This deflection changes the angle of reflection of a laser beam striking the cantilever, which is measured as the change in output from a photodetector.

The force–extension relationship of polymers need not, however, be solely entropic. AFM studies of certain glucopyranose polysaccharides showed that, while their elastic behavior was entropic under low force, a transition that occurs at higher force results in an increase in contour length[16–18]. This was shown to be due to the conversion of individual glucopyranose rings from the 'chair' conformation, which is energetically favoured at low force, to the longer 'boat' conformation[17]. An even more dramatic deviation from entropic elasticity is seen in the extension of multi-domain proteins. The force-extension curves of these proteins show peaks that correspond to the unfolding of single domains (Fig. 2b). As these proteins are elongated, the restoring force increases. At a certain force, however, one of the domains in the chain unfolds. Like the freeing of a tangle in a rope, this unravelling suddenly adds to the effective length of the protein and allows the force on the cantilever to fall to near zero. Further extension is resisted again by entropic forces until a second domain in the chain unravels. The force–extension curve therefore displays a characteristic saw-tooth pattern with the number of peaks corresponding to the number of domains stretched between the substrate and cantilever tip. This phenomenon was first demonstrated with titin[19] and later with the ECM protein tenascin[20,21], which contains repeats of the FN-III domain (Fig. 2c). The unfolding of each of the FN-III domains can be described accurately using the WLC model. The mean force at which the domains unfold is 137 pN and the mean interval between peaks is 24.8 ± 2.3 nm (Ref. 20).

AFM measurements offer an opportunity to understand the characteristics that underlie the mechanical properties of proteins. Elongation of the cytoskeletal protein spectrin (Fig. 3a), which contains repeated α-helical domains, results in a markedly different force–extension curve[22]. Unfolding occurs at much lower forces (25–35 pN) and the interval between peaks (31.7 ± 0.3 nm) reflects the larger number of amino acids within each spectrin domain[23]. Atomic force microscopy might thus allow for the distinction between mechanical topologies of different domain types. The extension of some proteins, however, leads to results that are more complex. Force–extension curves for a fragment of titin consisting of Ig domains 27–34 (Fig. 3b) revealed up to eight unfolding peaks (six in this example) at forces of 150–300 pN (Ref. 19). The height of the peaks tends to increase with each unfolding event, which suggests that domains have different mechanical stabilities and that those that are less mechanically stable unfold before those that are more stable. Furthermore, as will be discussed below, the early unfolding peaks show clear deviations from the entropic behaviour predicted by the WLC model. This force–extension curve thus illustrates an important drawback in the use of native protein fragments for the study of mechanical properties. When pulling a heterogeneous multi-domain protein, one usually cannot know which unfolding peak corresponds to which domain. The elastic properties of specific domains are therefore difficult, or impossible even, to identify. However, as discussed below, a solution to this problem has been provided by molecular biology.

Mechanical amplification by polyprotein engineering

Force–extension curves for small or single-fold proteins are difficult to interpret because non-specific interactions between the cantilever tip and the adsorbed protein layer can obscure the interactions of interest at short extensions, and their rupture might result in 'peaks' that resemble unfolding events. A regularly spaced saw-tooth pattern of peaks, however, is a clear indication that a single, multi-domain protein is being stretched. Recombinant proteins consisting of multiple repeats of a specific domain were therefore constructed. The first domain chosen for study was Ig domain I27 of titin[19] because it has a tertiary structure that is

well defined by NMR (Ref. 24), a known thermodynamic stability[25], and an unfolding pathway that has been modeled using steered molecular dynamics[26] (a method for predicting how a protein structure will respond to applied force). Polyproteins consisting of either eight or 12 repeats of this domain were cloned and expressed (Fig. 4a,b)[27]. Electron microscopic imaging of rotary shadowed $I27_{12}$ (12 repeats of Ig domain I27) demonstrated that these proteins have a rod-like structure with a length of ~58 nm (Fig. 4c), which is close to that expected based on NMR measurements of a single domain (4.4 nm) (Ref. 28). In contrast to the staircase pattern of unfolding peaks seen with titin (Fig. 3b), the force peaks for I27 unfolding were not ordered and were distributed around a single mean value of ~200 pN (Fig. 4d). The fitting of consecutive unfolding peaks according to the WLC model showed that each unfolding event added 28.4 ± 0.3 nm to the length of the protein. Protein engineering has therefore enabled precise measurements of the length increment caused by domain unfolding and of the mechanical stability of individual protein domains.

Kinetics of force-induced unfolding and refolding

The probability that a domain will unfold is dependent on the applied force, the extension required to break the bonds that hold the domain together and the rate at which the domain unfolds with no applied force (the equation describing this relationship is similar to that shown in Fig. 1). By modelling the probability of unfolding versus the applied force using Monte Carlo techniques, one can therefore estimate the unfolding distance and the unfolding rate at zero force[19,20,29]. The amplitude histogram for force-induced unfolding of I27 has been best modeled using an unfolding rate at zero force of 3.3×10^{-4} s^{-1} and an unfolding distance of 0.25 nm (Ref. 27). This suggests that unfolding of the I27 domain is triggered by extending it by the length of a single H_2O molecule. Similar unfolding rates were obtained by fitting a plot of unfolding forces versus the pulling speed of the AFM, which provided an independent estimate.

The AFM technique is also able to measure refolding of protein domains[19–22]. An extended protein can be relaxed by returning the substrate to its original position. Subsequent re-extension of the protein demonstrates a recovery of folded domains that is dependent on the time interval between consecutive extensions. A plot of refolding versus time for tenascin demonstrated that refolding occurs as the sum of at least two exponential rates, presumably because different domains have different rates of refolding[20]. The refolding of $I27_8$ (eight repeats of the Ig domain I27) domains, however, occurs at a single exponential rate of 1.2 s^{-1} (Ref. 27). This was the first mechanical

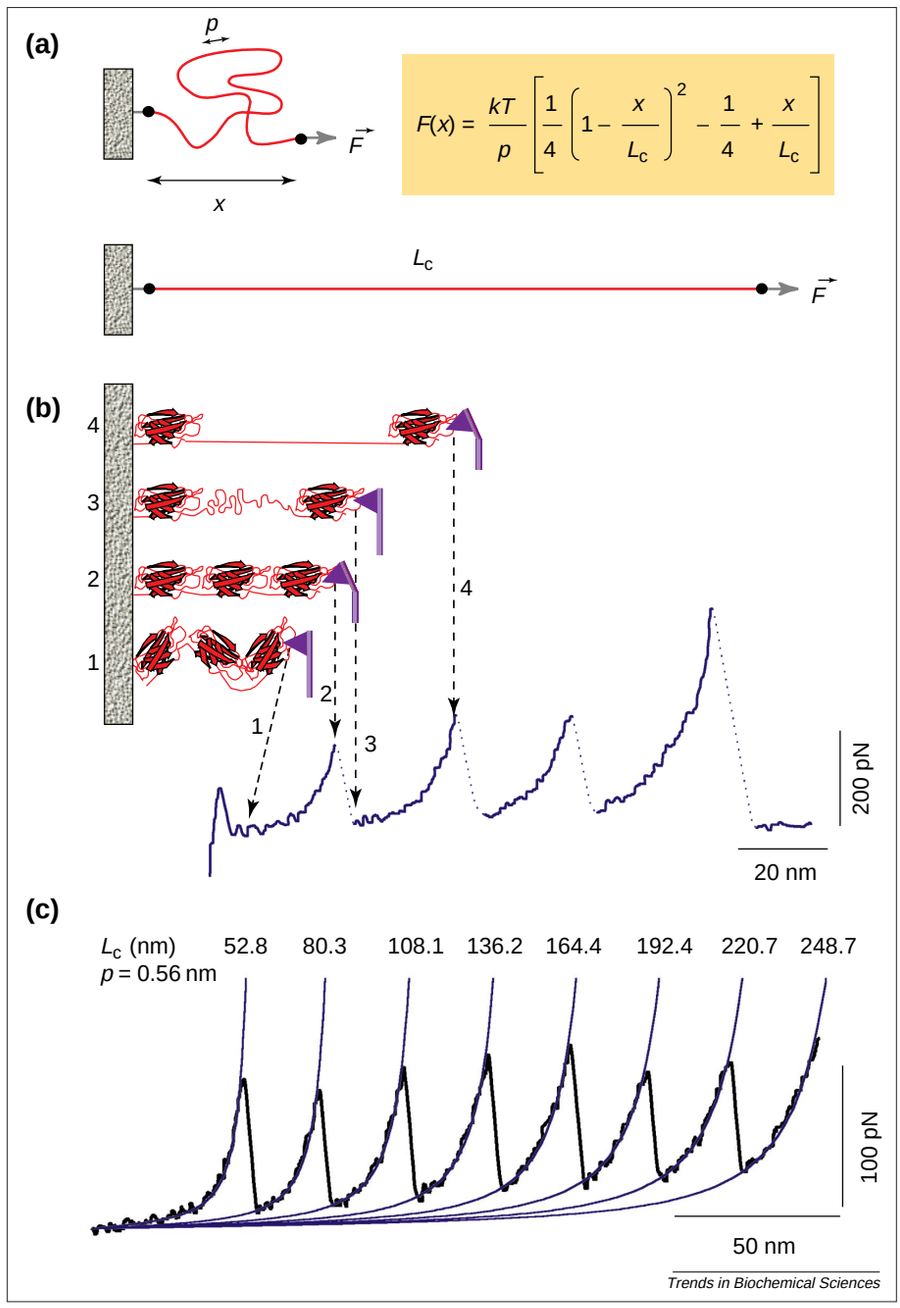

Figure 2

The entropic elasticity of proteins and domain unfolding. **(a)** The entropic elasticity of proteins can be described by the WLC (worm-like chain) equation (inset), which expresses the relationship between force (F) and extension (x) of a protein using its persistence length (p) and its contour length (L_C). k is Boltzmann's constant and T is the absolute temperature. **(b)** The saw-tooth pattern of peaks that is observed when force is applied to extend the protein corresponds to sequential unravelling of individual domains of a modular protein. As the distance between substrate and cantilever increases (from state 1 to state 2) the protein elongates, generating a restoring force that bends the cantilever. When a domain unfolds (state 3) the free length of the protein increases, returning the force on the cantilever to near zero. Further extension again results in force on the cantilever (state 4). The last peak represents the final extension of the unfolded protein prior to detachment from the AFM tip. **(c)** Consecutive unfolding peaks of recombinant human tenascin-C were fitted using the WLC model. The contour length (L_C) for each of the fits is shown; the persistence length (p) was fixed at 0.56 nm.

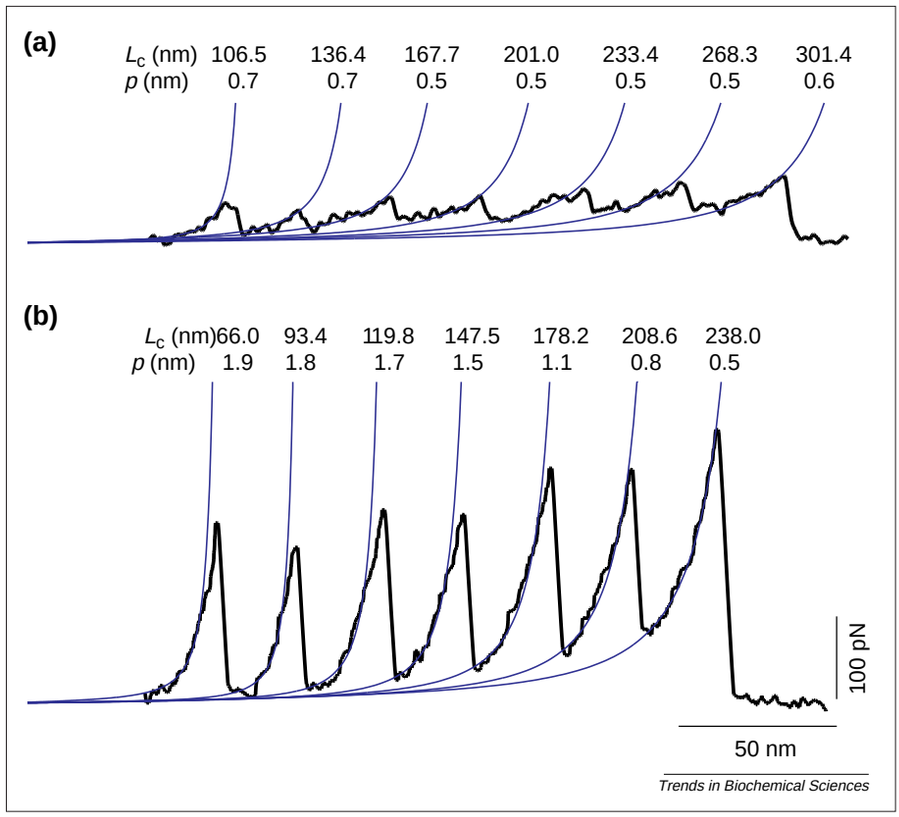

Figure 3

A comparison of force–extension curves for spectrin and titin. **(a)** A force–extension curve for the cytoskeletal protein spectrin showing the contour length and persistence length for each of the domains. (The trace shown was obtained using a recombinant fragment of β-spectrin containing the actin-binding domain and spectrin repeats 1–10, a kind gift from V. Bennett, Duke University.) **(b)** A force–extension curve for a recombinant fragment of titin consisting of titin Ig domains 27–34 showing the contour length (L_C) and persistence length (p) for each of the domains. Note that the early unfolding events deviate from the entropic behaviour predicted by the WLC (worm-like chain) model. The persistence length increases with each of the fits because for the early peaks, the flexibility of the protein is influenced by the size of the folded domains, whereas for the later peaks the flexibility is dominated by the individual bonds between amino acids.

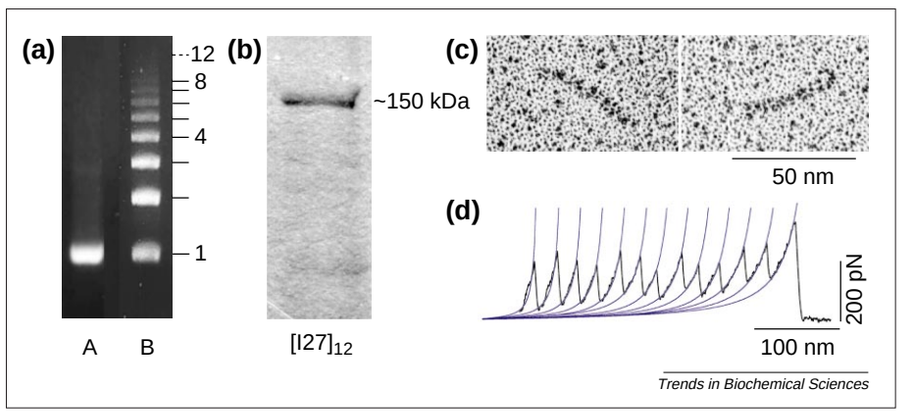

Figure 4

Construction and analysis of poly I27. **(a)** An illustration of the strategy for the construction of poly I27 protein using self-ligation of multiple copies of I27 cDNA monomers. Depicted is an agarose gel stained with ethidium bromide showing the I27 monomer (lane A) and a ladder of concatemers with various numbers of I27 monomers (lane B). For a detailed description of the method, see Ref. 27. **(b)** Coomassie blue staining of the purified $I27_{12}$ protein separated using SDS-PAGE. **(c)** Electron micrographs of rotary shadowed $I27_{12}$ (courtesy of Dr H. P. Erickson). Note the rod-like shape and the length of ~58 nm. **(d)** Fits of consecutive unfolding peaks of $I27_{12}$ using the WLC (worm-like chain) model. Note the random distribution of the unfolding forces for each peak and the deviation from entropic behaviour evident in the early peaks.

measurement of the refolding rate of an individual protein domain.

How do the AFM measurements of I27 unfolding and refolding kinetics compare with those obtained using chemical denaturation techniques? Guanidinium chloride denaturation techniques were used to estimate that the I27 domain unfolds at a rate of 4.9×10^{-4} s^{-1} in the absence of denaturant, a value very close to that derived from AFM experiments for unfolding in the absence of applied force (3.3×10^{-4} s^{-1}) (Ref. 27). The height of the unfolding energy barrier is therefore similar for the two methods (~22 kcal mol^{-1}). This suggests that both methods revealed a similar unfolding process, although it remains to be established whether this similarity is specific for mechanical proteins. The rates of refolding measured by the two methods were, however, clearly different. The refolding rate for $I27_8$ following chemical denaturation (32 s^{-1}) was much faster than that following force-induced extension (1.2 s^{-1}). This might be due to the tethering of I27 domains, which should decrease the rotational freedom of the molecule and might thereby inhibit the reformation of the folded structure. Because Ig and FN-III domains exist as parts of larger proteins, however, this slower rate of refolding might better reflect the process *in situ*.

Molecular determinants of an elastic domain

Recent studies have begun to explore the characteristics that define an elastic domain. The component β-strands of I27 (referred to as strands A through G) form two β-sheets (Fig. 5) that are held together by hydrogen bonds and by hydrophobic core interactions. One sheet consists of strands A, B, D and E, whereas the other is formed by a portion of strand A (A′), and strands C, F and G. This structure is stabilized by numerous hydrogen bonds between adjacent strands.

What determines the stability of the β-sandwich structure under mechanical stress? Steered molecular dynamics simulations of forced unfolding of I27 suggest that when force is applied to the C- and N-terminal strands the greatest resistance to unfolding is provided by a patch of hydrogen bonds between the A′ and G strands[26] (Fig. 5). This model is similar to that achieved by analysing the crystal structure of an Ig domain from intercellular adhesion molecule-1 (ICAM-1) (Ref. 30). This

arrangement means that the A′ and G strands must slide past one another for unfolding to occur. Because the bonds are perpendicular to the axis of extension, they must rupture simultaneously to allow relative movement of the two termini. This is stronger than an arrangement in which strands are perpendicular to the axis of extension, in which case hydrogen bonds would rupture consecutively, like the tabs of a zipper. Following rupture of the bonds connecting the A′ and G strands, the remainder of the fold unravels with little resistance.

This model fits well with experimental observations[27]. The short unfolding distance observed for I27 (0.25 nm) is consistent with the idea that unfolding occurs easily following the rupture of the hydrogen bonds in the A′–G patch. The number of amino acids in the I27 sequence between the A′ and G strand hydrogen bonds (72–78, depending on how it is counted) agrees well with the observed space between peaks (28.4 ± 0.3 nm), which predicts 75 amino acids in the I27 fold (75 × 0.38 nm = 28.5 nm). When mutant polyproteins were constructed with an extra five glycine residues within the fold, the interval between unfolding peaks was lengthened by ~1.91 nm per domain[31], which is close to the expected difference (5 × 0.38 nm = 1.90 nm). Insertion of glycine residues between the I27 folds does not alter the unfolding interval because these sections are fully stretched before unfolding occurs[31]. Furthermore, as the model implies, the final unfolding step occurs as a single event. If there were bonds positioned deeper within the fold that were approximately as strong as the A′–G bond, the unfolding of each domain would give multiple force peaks and the unfolding of multiple domains would be likely to occur in irregular, interspersed steps.

Despite the similarity in the chemical stability, spectrin domains unfold at much lower forces (25–35 pN)[22] than do those of titin[19] (150–300 pN) and tenascin[20] (a mean of 137 pN). Modelling of the forces involved in spectrin extension suggests that the unfolding distance for a spectrin α-helix is 1.5 nm, which is sixfold greater than that for titin I27 (0.25 nm)[27]. Because unfolding probability is exponentially dependent on the product of force and unfolding distance (see Fig. 1), this difference in unfolding distance might explain the observed difference in mechanical stability. The greater unfolding distance for spectrin is probably due to its tertiary structure. The α-helices of spectrin are maintained mainly by hydrophobic interactions, which are weaker and maintained over a greater distance than hydrogen bonds.

Unfolding intermediates and misfolding events

Molecular simulations[26] predict that rupture of the two hydrogen bonds between the A and B strands should occur prior to the disruption of the bonds between the A′ and G strands (Fig. 5). Breakage of these bonds at low force lengthens the I27 domain by about 15%, and might thus contribute an important component to the elasticity of titin. The force–extension curve of either titin[19] (Fig. 3) or poly-I27 (Ref. 27 and Fig. 4) reveals a deviation from entropic behaviour prior to domain unfolding, which corresponds to a lengthening of the I27 domain by the predicted 15% (Ref. 32). This deviation is particularly evident during the domains that unfold first and is likely to represent simultaneous breakage of the A–B bonds in each of the domains. The appearance of a smaller hump during the subsequent unfolding event suggests that the remaining domains rapidly return to their original conformation before the next unfolding event occurs. Such conformational changes prior to unfolding might also be important in regulating protein–protein interactions. A steered molecular dynamics simulation of forced unfolding of a FN-III domain suggests that deformation of the integrin-binding 'RGD' motif occurs during an early stage of domain extension[33]. The application of force might thereby cause a conformational change leading to the detachment of a bound integrin molecule from a FN-III domain. Thus, the RGD motif of FN-III might act as a mechanosensitive switch that controls the interaction between cell-adhesion molecules.

AFM refolding experiments have also identified misfolding of I27 domains[34]. Extension of refolded $I27_8$ rarely (2%) resulted in force–extension curves with peaks missing between apparently normal unfolding events ('skips'). The interval between the peaks before and after the skip corresponds to the size of two I27 domains plus the number of amino acids between I27 folds. Skips therefore appear to represent misfolding events in which the A strand of one domain interacts with the G strand of the adjacent domain, thereby creating a much larger fold that nevertheless has a stability similar to that of a native I27 fold.

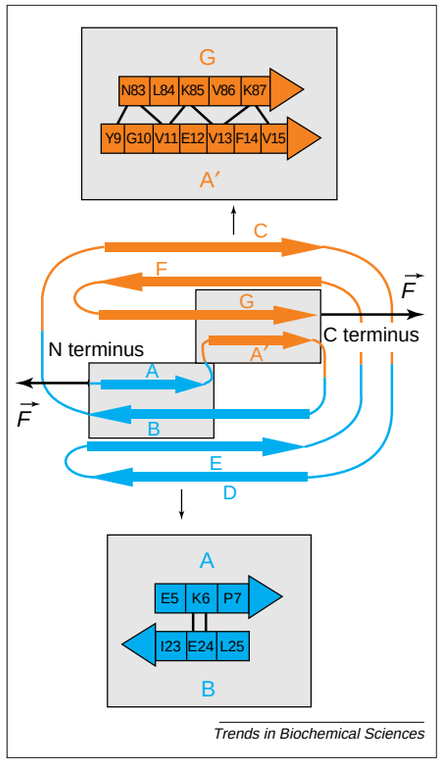

Figure 5

The mechanical topology of I27. A schematic diagram of the topology of the β-sandwich structure of I27. Each β-strand is shown as an arrow, with strands from the two β-sheets shown in different colours. The sites of interaction between the A′ and G strands and the A and B strands are shown on an expanded scale at the top and bottom, respectively. Amino acids, indicated by the single-letter code, are shown in the boxes and the hydrogen bonds between amino acids are indicated by the lines.

The energetics of force-induced unfolding and refolding

Current models describe the energy landscape for a folding protein as being similar to a funnel[35–37]. At the top of this funnel, proteins exist in a highly disordered, unfolded state of high energy and high entropy. Proteins are driven to assume progressively more ordered, lower energy conformations, until the native structure, with the lowest entropy and energy, is formed. The force-induced extension of a protein, however, has added implications. Under mechanical stress, the I27 domain is converted from its native conformation (N) to a condensed denatured state (CD), in which it is coiled but not folded (Fig. 6a). These conformations correspond to the energy states at the bottom and the top of the 'unfolding' funnel. A third state, the extended denatured state (ED), occurs only during mechanically induced unfolding. A different energy landscape is

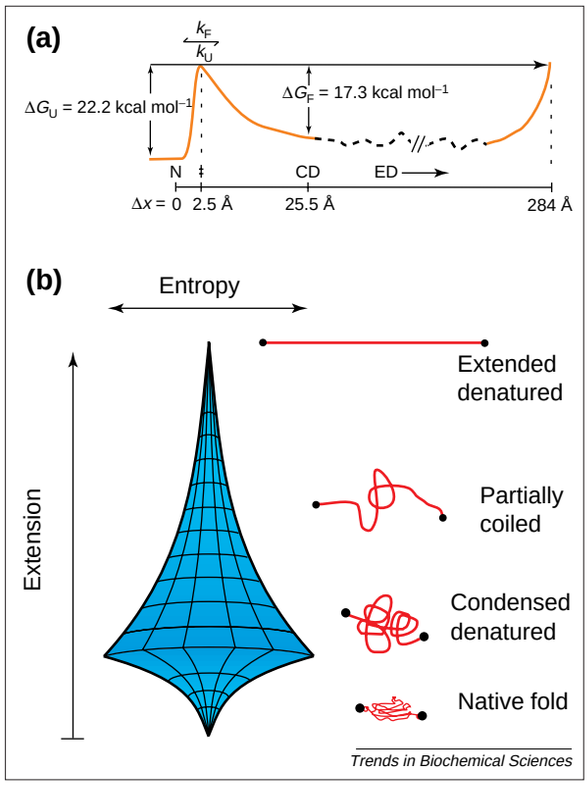

Figure 6

The energy landscape of force-induced unfolding and folding. **(a)** Force-induced unfolding (U) and folding (F) of the I27 domain, expressed as the change in free energy (ΔG_U and ΔG_F, respectively) as the molecule is extended. k_F and k_U refer to the rates of folding and unfolding, respectively. Extension of the native conformation (N) by only 2.5 Å brings the protein to a transition state (‡) at the height of the energy barrier between the folded and unfolded states. In the condensed denatured state (CD), the protein is coiled but not folded (Δx = 25.5 Å), whereas in the extended denatured state (ED), the protein has been forcibly extended towards its contour length (Δx = 284 Å). **(b)** A model describing the relationship between extension and entropy in force-induced unfolding. Diagrams on the right illustrate the conformations at different extensions. The entropy of the chain is near zero when the protein is nearly fully extended or in its native conformation, and is maximal when the protein is in its condensed denatured state.

therefore required to describe the relationship between extension of a protein and its entropy (Fig. 6b). A fully extended protein has an entropy of near zero. When the protein is freed from mechanical restraint, it is driven by entropic forces to its condensed denatured state. The protein then assumes its energetically favoured native fold (Fig. 6a) and, again, has an entropy of near zero. A model of the relationship between entropy and length might therefore appear more like a 'top' than a 'funnel', with the addition of an elongated and inverted second 'funnel'. The long upper curve represents the force-induced extension of the protein and its entropy-driven recoiling when the force is relaxed. The funnel-shaped bottom represents the smaller change in length that occurs as the protein assumes its native conformation. This model offers a more complete description of the energetics of unfolding and refolding of individual domains tethered in proteins exposed to force-induced extension.

Conclusion

The AFM offers a novel and direct means to measure the mechanical properties of biological polymers. In combination with techniques from molecular and structural biology, the AFM will help to elucidate the determinants of the mechanical stability of protein domains. The AFM will also allow an unprecedented glimpse at the mechanics of protein–protein interactions. These techniques can be applied to diverse mechanical systems such as those underlying the extracellular matrix, muscle elasticity, molecular motors and the exocytotic fusion apparatus.

Acknowledgement

This work was funded by R01 grants from the National Institutes of Health to J. M. Fernandez.

References

1 Chothia, C. and Jones, E. Y. (1997) *Annu. Rev. Biochem.* 66, 823–862
2 Chicurel, M. E., Chen, C. S. and Ingber, D. E. (1998) *Curr. Opin. Cell Biol.* 10, 232–239
3 Bork, P. and Doolittle, R. F. (1992) *Proc. Natl. Acad. Sci. U. S. A.* 89, 8990–8994
4 Erickson, H. P. (1994) *Proc. Natl. Acad. Sci. U. S. A.* 91, 10114–10118
5 Ohashi, T., Kiehart, D. P. and Erickson, H. P. (1999) *Proc. Natl. Acad. Sci. U. S. A.* 96, 2153–2158
6 Hocking, D. C., Sottile, J. and McKeown-Longo, P. J. (1994) *J. Biol. Chem.* 269, 19183–19187
7 Morla, A., Zhang, Z. and Ruoslahti, E. (1994) *Nature* 367, 193–196
8 Ingham, K. C., Brew, S. A., Huff, S. and Litvinovich, S. V. (1997) *J. Biol. Chem.* 272, 1718–1724
9 Zhong, C. *et al.* (1998) *J. Cell Biol.* 141, 539–551
10 Binnig, G., Quate, C. F. and Gerber, C. (1986) *Phys. Rev. Lett.* 56, 930–933
11 Rief, M., Fernandez, J. M. and Gaub, H. E. (1998) *Phys. Rev. Lett.* 81, 4764–4767
12 Engel, A., Gaub, H. E. and Muller, D. J. (1999) *Curr. Biol.* 9, R133–R136
13 Flory, P. J. (1989) *Statistical Mechanics of Chain Molecules*, Hanser Publishers
14 Bustamante, C., Marko, J. F., Siggia, E. D. and Smith, S. (1994) *Science* 265, 1599–1600
15 Marko, J. F. and Siggia, E. D. (1995) *Macromolecules* 28, 8759–8770
16 Rief, M., Oesterhelt, F., Heymann, B. and Gaub, H. E. (1997) *Science* 275, 1295–1297
17 Marszalek, P. E., Oberhauser, A. F., Pang, Y. P. and Fernandez, J. M. (1998) *Nature* 396, 661–664
18 Marszalek, P. E. *et al. Proc. Natl. Acad. Sci. U. S. A.* (in press)
19 Rief, M. *et al.* (1997) *Science* 276, 1109–1112
20 Oberhauser, A. F., Marszalek, P. E., Erickson, H. P. and Fernandez, J. M. (1998) *Nature* 393, 181–185
21 Rief, M., Gautel, M., Schemmel, A. and Gaub, H. E. (1998) *Biophys. J.* 75, 3008–3014
22 Rief, M., Pascual, J., Saraste, M. and Gaub, H. E. (1999) *J. Mol. Biol.* 286, 553–561
23 Speicher, D. W. and Marchesi, V. T. (1984) *Nature* 311, 177–180
24 Improta, S., Politou, A. S. and Pastore, A. (1996) *Structure* 4, 323–337
25 Politou, A. S., Thomas, D. J. and Pastore, A. (1995) *Biophys. J.* 69, 2601–2610
26 Lu, H. *et al.* (1998) *Biophys. J.* 75, 662–671
27 Carrion-Vazquez, M. *et al.* (1999) *Proc. Natl. Acad. Sci. U. S. A.* 96, 3694–3699
28 Improta, S. *et al.* (1998) *J. Mol. Biol.* 284, 761–777
29 Kellermayer, M. S., Smith, S. B., Granzier, H. L. and Bustamante, C. (1997) *Science* 276, 1112–1116
30 Casasnovas, J. M. *et al.* (1998) *Proc. Natl. Acad. Sci. U. S. A.* 95, 4134–4139
31 Carrion-Vazquez, M. *et al. Proc. Natl. Acad. Sci. U. S. A.* (in press)
32 Marszalek, P. E. *et al. Nature* (in press)
33 Krammer, A. *et al.* (1999) *Proc. Natl. Acad. Sci. U. S. A.* 96, 1351–1356
34 Oberhauser, A. F., Marszalek, P. E., Carrion-Vasquez, M. and Fernandez, J. M. *Nat. Struct. Biol.* (in press)
35 Onuchic, J. N., Luthey-Schulten, Z. and Wolynes, P. G. (1997) *Annu. Rev. Phys. Chem.* 48, 545–600
36 Chan, H. S. and Dill, K. A. (1998) *Proteins* 30, 2–33
37 Matagne, A. and Dobson, C. M. (1998) *Cell. Mol. Life Sci.* 54, 363–371
38 Bell, G. I. (1978) *Science* 200, 618–627
39 Evans, E. and Ritchie, K. (1997) *Biophys. J.* 72, 1541–1555